

Brilliantly Red: The Structure of Carmine

Erik Svensson Grape,* Tom Willhammar, and A. Ken Inge

Cite This: *Cryst. Growth Des.* 2025, 25, 4100–4105

Read Online

ACCESS |



Metrics & More

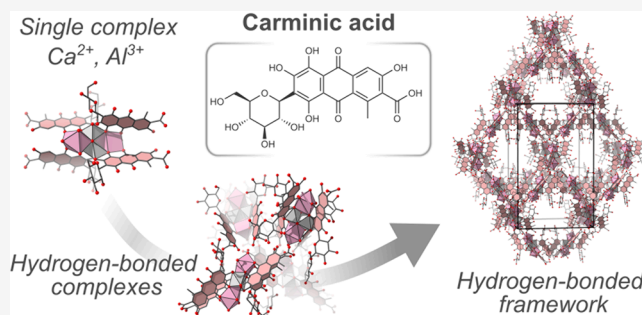


Article Recommendations



Supporting Information

ABSTRACT: Carmine is a red pigment made from dried cochineal, a scale insect that has been a source of brilliant scarlet reds in clothing and art for more than two millennia, with records dating back to 700 BC. Since the 16th century, it has been intensely traded all over the world and was one of the most important trade goods for the Spanish empire at its economic peak. Despite still being used on an industrial scale, with hundreds of metric tonnes produced annually, the exact molecular and crystal structures of the dyestuff remains undetermined. Notably, both modern-day commercial carmine and pigments prepared following historical recipes show strikingly similar diffraction patterns, indicating a common crystalline structure. Here we show that the crystal structure of carmine can, at last, be determined using three-dimensional electron diffraction measurements, revealing a tetranuclear complex that assembles into a nanoporous supramolecular structure with pore diameters of approximately 1.8 nm, held together by intermolecular hydrogen bonding. Our results establish a definite structure of carmine, unveiling a surprisingly complicated arrangement in a long-used commodity with economic and cultural impact, while also highlighting the serendipitous creation of a man-made supramolecular material that dates back hundreds if not thousands of years.



Throughout history, few colors have evoked such a sense of power and prestige as red—associated in many cultures with warmth, love, and desire, but also blood, war, and sacrifice. During the European medieval and Renaissance eras, brilliant red pigments were greatly sought after and a costly color to wear. Indicative of great wealth and power, garments of crimson and scarlet hues were almost exclusively worn by aristocrats and members of royal families.¹ The high status of red was largely a consequence of the scarcity of the pigments themselves: while madder root (*Rubia tinctorum*) dyes—which could exhibit colors from red to orange—were relatively common in past centuries, obtaining strong shades of red from the root was an arduous process that remained a trade secret between dyers of the Ottoman empire.¹ Alternative sources of striking scarlets and crimson hues at the time included brazilwood (*Paubrasilia echinata*) as well as various insects that were used to produce pigments such as kermes (specifically the insect *Kermes vermilio*), St. John's blood (obtained from *Porphyrophora polonica*), and Armenian red (*Porphyrophora hameli*). The latter two were considered some of the finest red dyestuffs at the time, which combined with the scarcity of the insects due to hardships in their cultivation made the pigments incredibly valuable. However, it turned out that native Peruvians had developed a spectacular and far more powerful red dye. In the early 1500s, as Spanish conquistadors reached America, this very limited supply chain was disrupted, opening the door to a dyestuff that would be transported and traded across the world for centuries to come, making a long-standing

impact on art and culture,² and completely replacing the prior use of St. John's blood and Armenian red.³

The source of this spectacular dye was cochineal (Figure 1a), a scale insect closely related to those from which St. John's blood and Armenian red are sourced. The stationary females of the species live on and feed off of cacti, and would be easy prey for a range of predators, were it not for the strongly colored deterrent they produce: carminic acid (Figure 1b). Carmine—the pigment derived from carminic acid—was central to many people of ancient America,¹ and evidence for its presence been found in samples that are over 2,000 years old.³ Through breeding and harvesting cochineal for centuries, the species now classified as *Dactylopius coccus* came to be—the females of which are significantly larger than their wild ancestors and contain >20 wt % carminic acid.⁴ The cultivation of cochineal favorably took place in the highlands of southern Mexico, owing to the dry and warm climate of the region.

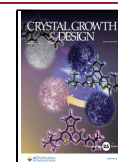
Historically, preparation of carmine involved drying and grinding cochineal and subsequently extracting carminic acid (Figure 1c). To precipitate carminic acid from aqueous solutions, a mordant would be used—typically a colorless

Received: February 13, 2025

Revised: May 20, 2025

Accepted: May 21, 2025

Published: June 3, 2025



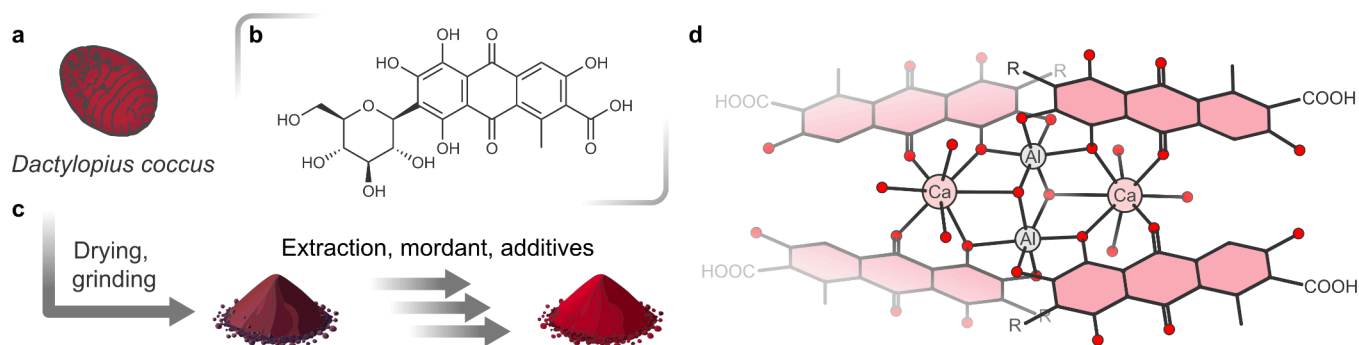


Figure 1. (a) Sketch of the domesticated cochineal (*Dactylopius coccus*), adapted from illustrations made by Nicolaas Hartsoecker in 1694.⁸ (b) Carminic acid, the colorful molecule produced by the cochineal. (c) Schematic illustration of carminic acid extraction from dried and ground cochineal (dark red to black in color) and preparation of carmine pigment through the addition of a mordant, typically alum (potassium aluminum sulfate), affording a brilliantly red powder. (d) The tetranuclear molecular complex of carmine as determined by three-dimensional electron diffraction measurements, showing carminate dianions coordinating to octahedral Al^{3+} cations and square antiprismatic Ca^{2+} cations (oxygen: red spheres), with two deprotonated phenol groups chelating toward the aluminum cations ($\text{R} = \text{glucose}$). The tetranuclear unit is also held together by bridging hydroxide anions, giving a charge-balanced motif, where the three oxygens coordinating toward each calcium are attributed to water molecules.

inorganic substance. Being common reagents in the production of pigments and dyes, mordants induce aggregation, creating precipitates known as lake pigments: products of low solubility and high fastness that attach to fabrics or can be filtered off.⁵ While detailed historic recipes are few and hard to come by, one of the most commonly used and naturally occurring mordants is alum (potassium aluminum sulfate), which was used by Aztec dyers to make carminic acid adhere to their fabrics.¹

Farming of cochineal and production of carmine would prove a profitable endeavor for centuries, and the annual import of cochineal to Spain averaged more than 100 metric tonnes by the end of the 1500s.⁶ Two decades later, in 1803, cochineal exports were valued at more than two million pesos, corresponding to roughly 30% of silver exports, making it one of the most valuable trade goods for the Spanish empire at the time.⁷ Carmine is still used today in a range of applications, particularly as a natural alternative to synthetic red dyes, and is listed in Europe as additive E120 when used in food. The production of pure carmine in recent years fluctuates between 20–50 metric tonnes in Peru alone,⁸ with a global cochineal production of ~800 metric tonnes annually.⁹

Due to its widespread historic and present-day use, the actual structure of carmine, and a possible explanation for its particular brilliance and fastness, has seen much speculation. Detailed investigations of carmine have so far included solid-state nuclear magnetic resonance (NMR) and mass spectrometry measurements.¹⁰ Single-crystal X-ray diffraction (SCXRD) studies of other pigments based on molecules of related structures have been performed, but not on carmine due to difficulties in growing sufficiently large crystals of the long-used dyestuff.¹¹ This lack of a structural and compositional understanding not only hinders the identification of carmine in historical samples or present-day products, but also impacts its use as a biological staining agent: carmine and carmine-derived staining agents are frequently used in histological applications, where it has been observed that variations in composition can compromise the overall staining processes.^{12,13} Notably, different carmine and carmine-derived formulations are used to stain different tissues or biochemical targets, highlighting the importance of understanding their

structure and composition, and ultimately what interactions govern the staining process for which they are used.¹⁴

Several models of carmine have been proposed, with previous investigations hinting at a tetranuclear structure containing four carminic acid molecules and some oxygen species, as well as calcium and aluminum cations, in a proposed ratio of 2:1:1 between carminic acid, calcium, and aluminum.^{10,13} Notably, evidence suggests that particularly bright-red ‘crimson lake’ is only obtained when both calcium and aluminum ions are present, while purple hues are obtained using alternative preparation methods lacking calcium.¹⁵ Such an effect has also been observed for madder lake pigments, in which cation identities have been observed to influence the color of the pigment by modifying the charge distribution within the complex.¹¹ Even so, the exact arrangement of the constituents of carmine remained unknown. In particular, the coordination environments of the aluminum and calcium cations and their bonding to the carminate dianions remains ambiguous, as does the identity and arrangement of different oxygen species in the form of either hydroxide or coordinated water molecules.^{12,10,8}

Using state-of-the-art electron crystallography methods, as described below, we present the molecular and crystal structure of carmine, unveiling a complex in which a core of two aluminum cations and two calcium cations are bridged by hydroxide groups, forming a butterfly shaped motif (Figure 1d), similar to that observed in previously described alizarin dyes.¹¹ The pairs of phenolate groups on the carminic acid molecules are found to be chelating to the Al^{3+} cations, and one of the phenolates and one anthraquinone carbonyl chelate to the Ca^{2+} , which concur with previous spectroscopic measurements,¹⁰ while the carboxylic acid group and its neighboring phenol group remain uncoordinated. This confirms the speculated 2:1:1 ratio between carminic acid, calcium, and aluminum. However, as detailed below, there is more to the structure of carmine than the complex itself, such as its intermolecular interactions, that result in a rather unexpected crystal structure.

First, to put the structure of carmine into context, one needs to prepare the pigment in a historically relevant manner. A great source of historical recipes for dyes and pigments is the archives of the British manufacturer Winsor & Newton,

founded in 1832, which to this day specializes in fine art products, including so-called lake pigments such as carmine. The Winsor & Newton Archive of 19th Century Artist's Materials contains recipe books and process records from the company's activities during the 19th century and includes a total of 443 records pertaining to cochineal products.¹⁵ The main manufacturing method used by Winsor & Newton, labeled "Finest Orient Carmine", involves grinding dried cochineal and extracting the carminic acid under acidic conditions (see details in the [Supporting Information](#)).¹⁵ Milk, boric acid (presumably used as a buffer), and alum are then added in succession to the obtained deep-red filtrate, ultimately yielding a brilliantly red and crystalline precipitate, as confirmed by powder X-ray diffraction ([Figure 2a](#), 19th-

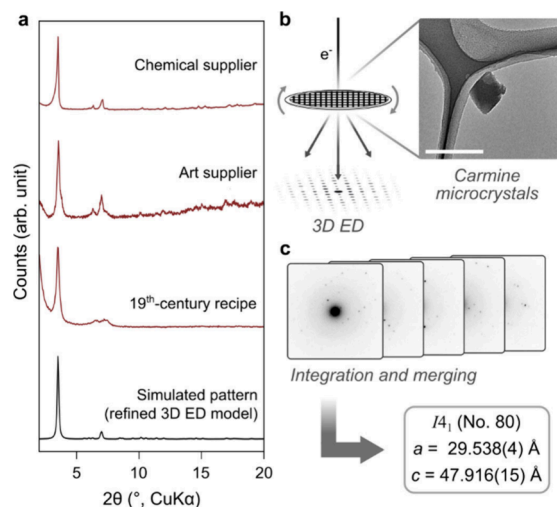


Figure 2. (a) Powder X-ray diffraction (PXRD) patterns of carmine from various sources as well as the simulated pattern from the structure determined by three-dimensional electron diffraction (3D ED). (b) Schematic illustration of the collection of 3D ED data, as well as a transmission electron microscopy image of a carmine crystal (chemical supplier) on a holey carbon-covered copper grid (scale bar, 0.5 μm). (c) Integration and merging of electron diffraction data, as well as unit cell parameters after further refinement against PXRD data, corresponding to a unit cell volume of 41,805(17) \AA^3 .

century recipe). Notably, carmine was purchased from different sources, including modern-day chemical and art suppliers (see the [Supporting Information](#) for details); they were also crystalline and exhibited strikingly similar X-ray powder diffraction patterns compared to the sample prepared from the historic recipe ([Figure 2a](#)), indicating that they possess a common crystal structure.

Considering the apparent crystalline nature of carmine and its composition—a naturally occurring and phenol-bearing organic molecule combined with metal cations—other historically relevant formulations and materials come to mind, such as iron gall inks¹⁶ and bismuth subsalicylate,¹⁷ the structures of which have only recently been elucidated. A growing class of modern-day materials of similar composition are metal–organic frameworks and metal-bearing hydrogen-bonded organic frameworks—crystalline porous materials that have garnered attention for a large range of applications.^{18,19} In such framework-type materials, a central concept is the supramolecular assembly of the constituent building units into porous structures, yet they can often only be obtained as microcrystalline powders, and elucidation of their structures is

often a challenging task.²⁰ However, continuous advancements in characterization methods lead to new insights across all branches of the physical sciences, including studies of atomic-scale arrangements. Of particular relevance to microcrystalline compounds and studies of the long-range order within them is the transmission electron microscopy (TEM) technique of three-dimensional electron diffraction (3D ED),²¹ also known as microcrystal electron diffraction (microED). The technique allows for the collection of single-crystal diffraction data from micro- and nanocrystalline samples ([Figure 2b](#)) and has proven powerful for determining the crystalline arrangements of samples previously difficult to characterize due to their small crystallite sizes, including pharmaceuticals,^{22–24} macromolecules,^{25–27} and materials.^{28,29} Notably, electron diffraction techniques has been used to aid in the structural characterization of a range of synthetic pigments of commercial significance.^{30–32}

To determine the structure of carmine and shed light on the composition and underlying structure of this long-used pigment, the sample that appeared most well-diffracting was chosen for 3D ED measurements ([Figure 2a](#), chemical supplier). Once inside the electron microscope, the bright red powder was revealed to be comprised of microcrystals (0.3–0.6 μm) that exhibit a pseudo-octahedral morphology ([Figure 2b](#), [Figure S1](#)). Several 3D ED data sets were collected at a temperature of 98 K ([Table S1](#), [Figure S2](#); see the [Supporting Information](#) for details) and could successfully be indexed to a body-centered tetragonal lattice. With a unit cell volume larger than 40,000 \AA^3 ([Figure 2c](#)), the volume of the repeating unit approaches those typically seen for macromolecules, indicating the presence of large structural motifs. Structure solution from the 3D ED data revealed that carmine is indeed built up by butterfly shaped tetranuclear units, as illustrated in [Figure 1d](#).^{10,11} As aforementioned, the coordination of the carminate dianions to the aluminum and calcium cations in the structure occurs through the catechol and quinone oxygens rather than the carboxylic acid groups. These functional groups chelate the cations and likely form stronger metal–ligand interactions with the trio of oxygens permitting a doubly chelating motif. Such a preference of phenolate over carboxylate has also been observed in structures containing gallic acid,^{33,34} another naturally occurring molecule bearing both phenol and carboxylic acid functional groups. The coordination environment of the aluminum and calcium cations in carmine are completed by bridging hydroxide groups at the center of the tetranuclear complex, as well as water molecules coordinating toward the calcium cations, yielding aluminum and calcium cations in octahedral and square antiprismatic coordination environments, respectively. This gives a molecular formula of $\text{Al}_2(\text{OH})_2(\text{C}_{22}\text{H}_{18}\text{O}_{13})_4\text{Ca}_2(\text{H}_2\text{O})_6$. The composition was also confirmed by energy-dispersive X-ray spectroscopy (see the [Supporting Information](#) for details), indicating an aluminum and calcium content in agreement with that expected (0.89 atom % each, excluding hydrogen content) from the determined structure (0.97 ± 0.1 atom % aluminum, 1.04 ± 0.1 atom % calcium, excluding hydrogen content).

The most striking feature of the solid-state structure of carmine is the arrangement of the tetranuclear units, forming a supramolecular framework with voids that are ~ 18 \AA across at their maximum width ([Figure 3](#)), with aperture sizes of 13 \AA . This occurs as four carmine units meet at what may be best described as hydrogen-bonded nodes in the structure ([Figure](#)

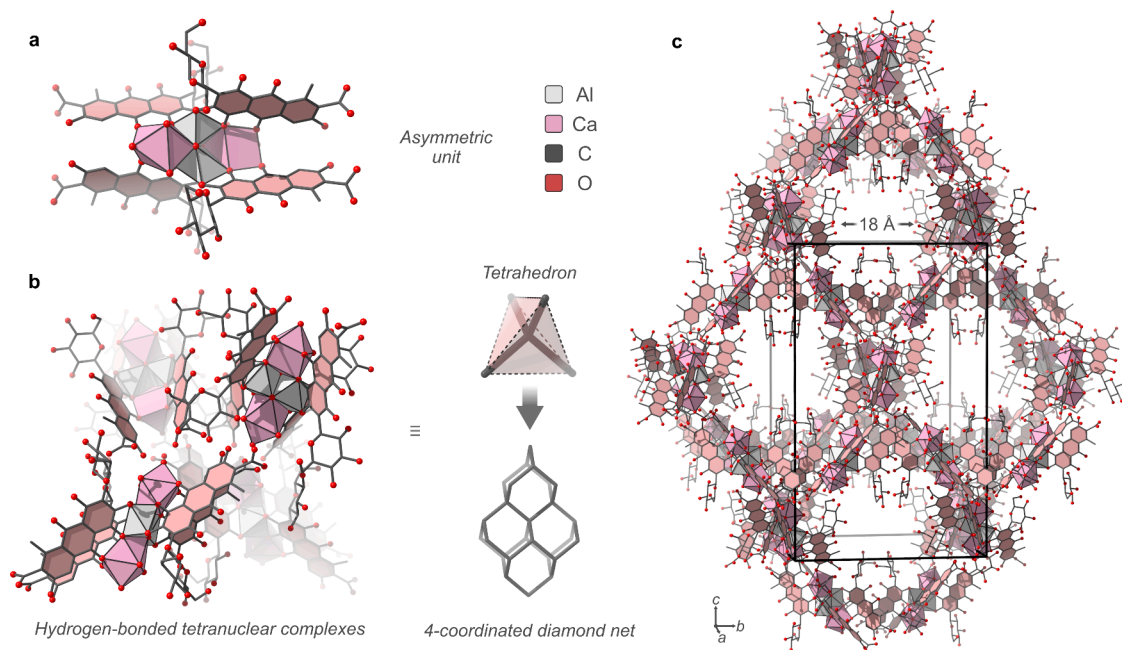


Figure 3. (a) Asymmetric unit of the crystal structure of carmine. (b) Assembly of four tetranuclear units, forming hydrogen-bonded nodes approximating a tetrahedral shape, leading to the diamond-like connectivity of the structure, with edges of the net coinciding with the tetranuclear complex. (c) View of the supramolecular structure of carmine, showing a hydrogen-bonded arrangement that results in a structure with 18 Å wide pores (solvent molecules have been excluded for clarity). Black lines: unit cell.

3b), forming tetrahedron-like units held together by up to 30 hydrogen bonds at their center (Figure S4), stabilizing the porous structure. Topologically, the connectivity of the supramolecular arrangement, comprised of four-coordinated tetrahedron-like units, is the same as that of diamond (Figure 3b).³⁵

The structure model initially obtained by 3D ED measurements could successfully be refined against powder X-ray diffraction (PXRD) data collected on the same sample (Figure S3 and Table S2), further validating the structure. It should be noted that the PXRD data show significant reflections to a limited resolution (~ 3 Å, Figure S3) and only permit refinement of the carminate dianions as rigid bodies. However, taken together with the structure solution from 3D ED and previous results from spectroscopic investigations,¹⁰ the refinement serves to validate the structure on a bulk scale. This also shows that the characteristic low-angle peak in the PXRD pattern, at $2\theta \approx 3.5^\circ$ (Cu $K\alpha$ radiation, Figure 2a), can be used as a fingerprint-like indication of crystalline calcium–aluminum carmine being present in a sample. This effectively paves the way for a noninvasive and precise characterization method for identifying carmine pigment in both commercial and historical samples, especially considering the non-destructive nature of X-ray diffraction measurements. Additionally, establishing a well-defined crystal structure and composition of crystalline carmine could aid also regulatory matters in commerce, possibly distinguishing pigments of different qualities and origins.⁴

Considering the long history of carmine production,^{36,37} the complexity of its supramolecular structure is surprising, as modern-day chemists have only in the last handful of decades started to categorize supramolecular assemblies and the formation of framework-type materials, as well as their interactions with other matter, including biomolecules and textiles.^{38,39} This shows that complex supramolecular structures and nanoporous materials have been synthesized

hundreds or perhaps even thousands of years ago; we only just recently started to look for and consciously create them.

■ ASSOCIATED CONTENT

Data Availability Statement

All diffraction and transmission electron microscopy data are available through the data repository Zenodo, including powder X-ray diffraction patterns, three-dimensional electron diffraction data sets, and micrographs. DOI: 10.5281/zenodo.14278562 and 10.5281/zenodo.14933194.

Supporting Information

The Supporting Information is available free of charge at <https://pubs.acs.org/doi/10.1021/acs.cgd.5c00185>.

Materials information and synthesis procedures, method descriptions, scanning electron micrographs, transmission electron micrographs, and PXRD patterns (PDF)

3D view of the carmine crystal structure (AVI)

Accession Codes

Deposition Number 2371686 contains the supplementary crystallographic data for this paper. These data can be obtained free of charge via the joint Cambridge Crystallographic Data Centre (CCDC) and Fachinformationszentrum Karlsruhe [Access Structures service](#).

■ AUTHOR INFORMATION

Corresponding Author

Erik Svensson Grape – Department of Chemistry and Biochemistry, Materials Science Division, University of Oregon, Eugene, Oregon 97403, United States; Department of Chemistry - Ångström Laboratory, Uppsala University, 75120 Uppsala, Sweden; Wallenberg Initiative Materials Science for Sustainability, Department of Chemistry, Stockholm University, 10691 Stockholm, Sweden;

orcid.org/0000-0002-8956-5897; Email: erik.svensson-grape@kemi.uu.se

Authors

Tom Willhammar – Wallenberg Initiative Materials Science for Sustainability, Department of Chemistry, Stockholm University, 10691 Stockholm, Sweden; orcid.org/0000-0001-6120-1218

A. Ken Inge – Wallenberg Initiative Materials Science for Sustainability, Department of Chemistry, Stockholm University, 10691 Stockholm, Sweden; orcid.org/0000-0001-9118-1342

Complete contact information is available at:
<https://pubs.acs.org/10.1021/acs.cgd.5c00185>

Notes

The authors declare no competing financial interest.

ACKNOWLEDGMENTS

E.S.G. acknowledges support from the Swedish Research Council (grant no. 2022-06178). The authors thank Marei Hacke and Anna Javér for fruitful discussion on historical pigments, and Richard W. Dapson for providing valuable insights into the role of carmine in biological staining processes.

REFERENCES

- (1) Greenfield, A. B. *A Perfect Red: Empire, Espionage, and the Quest for the Color of Desire*, 1st Harper Perennial ed.; Harper Perennial: 2006.
- (2) *A Red like No Other: How Cochineal Colored the World*; Padilla, C., Museum of International Folk Art, Eds.; Skira Rizzoli: 2015.
- (3) Wouters, J.; Rosario-Chirinos, N. Dye Analysis of Pre-Columbian Peruvian Textiles With High-Performance Liquid Chromatography and Diode-Array Detection. *J. Am. Inst. Conserv.* **1992**, *31* (2), 237–255.
- (4) Lloyd, A. G. Extraction and Chemistry of Cochineal. *Food Chem.* **1980**, *5* (1), 91–107.
- (5) Kirby, J.; Spring, M.; Higgit, C. The Technology of Red Lake Pigment Manufacture: Study of the Dyestuff Substrate. *National Gallery Technical Bulletin* **2005**, *26*, 71–87.
- (6) *From Silver to Cocaine: Latin American Commodity Chains and the Building of the World Economy, 1500–2000: Chapter 3 - Demand for American Dyes, 1550–1850*; Topik, S., Marichal, C., Frank, Z., Eds.; Duke University Press: 2006. DOI: 10.2307/j.ctv125jnbx.
- (7) Lee, R. L. Cochineal Production and Trade in New Spain to 1600. *Americas* **1948**, *4* (4), 449–473.
- (8) Müller-Maatsch, J.; Gras, C. The “Carmine Problem” and Potential Alternatives. In *Handbook on Natural Pigments in Food and Beverages*; Elsevier: 2016; pp 385–428. DOI: 10.1016/B978-0-08-100371-8.00018-X.
- (9) Frandsen, R. J. N.; Khorsand-Jamal, P.; Kongstad, K. T.; Nafisi, M.; Kannangara, R. M.; Staerk, D.; Okkels, F. T.; Binderup, K.; Madsen, B.; Møller, B. L.; Thrane, U.; Mortensen, U. H. Heterologous Production of the Widely Used Natural Food Colorant Carmine in *Aspergillus nidulans*. *Sci. Rep.* **2018**, *8* (1), No. 12853.
- (10) Harris, M.; Stein, B. K.; Tyman, J. H. P.; Williams, C. M. The Structure of the Colourant/Pigment, Carmine Derived from Carmine Acid. *J. Chem. Res.* **2009**, *2009* (7), 407–409.
- (11) Wunderlich, C.; Bergerhoff, G. Konstitution Und Farbe von Alizarin- Und Purpurin-Farblacken. *Chem. Ber.* **1994**, *127* (7), 1185–1190.
- (12) Dapson, R. W. The History, Chemistry and Modes of Action of Carmine and Related Dyes. *Biotechnol. & Histochemistry* **2007**, *82* (4–5), 173–187.
- (13) Meloan, S. N.; Valentine, L. S.; Puchtler, H. On the Structure of Carmine Acid and Carmine. *Histochemie* **1971**, *27* (2), 87–95.
- (14) Titford, M. Progress in the Development of Microscopical Techniques for Diagnostic Pathology. *J. Histochem. Technol.* **2009**, *32* (1), 9–19.
- (15) Vitorino, T. M. F. *A Closer Look at Nineteenth Century Cochineal Lake Pigments Through Historical Recipes Reconstructions*; Universidade Nova de Lisboa: 2020.
- (16) Ponce, A.; Brostoff, L. B.; Gibbons, S. K.; Zavalij, P.; Viragh, C.; Hooper, J.; Alnemrat, S.; Gaskell, K. J.; Eichhorn, B. Elucidation of the Fe(III) Gallate Structure in Historical Iron Gall Ink. *Anal. Chem.* **2016**, *88* (10), 5152–5158.
- (17) Svensson Grape, E.; Rooth, V.; Nero, M.; Willhammar, T.; Inge, A. K. Structure of the Active Pharmaceutical Ingredient Bismuth Subsalicylate. *Nat. Commun.* **2022**, *13* (1), 1984.
- (18) Furukawa, H.; Cordova, K. E.; O’Keeffe, M.; Yaghi, O. M. The Chemistry and Applications of Metal-Organic Frameworks. *Science* **2013**, *341* (6149), No. 1230444.
- (19) Zhu, Z.-H.; Wang, H.-L.; Zou, H.-H.; Liang, F.-P. Metal Hydrogen-Bonded Organic Frameworks: Structure and Performance. *Dalton Trans.* **2020**, *49* (31), 10708–10723.
- (20) Huang, Z.; Willhammar, T.; Zou, X. Three-Dimensional Electron Diffraction for Porous Crystalline Materials: Structural Determination and Beyond. *Chem. Sci.* **2021**, *12* (4), 1206–1219.
- (21) Gemmi, M.; Mugnaioli, E.; Gorelik, T. E.; Kolb, U.; Palatinus, L.; Boullay, P.; Hovmöller, S.; Abrahams, J. P. 3D Electron Diffraction: The Nanocrystallography Revolution. *ACS Cent. Sci.* **2019**, *5* (8), 1315–1329.
- (22) Gruene, T.; Wennmacher, J. T. C.; Zaubitzer, C.; Holstein, J. J.; Heidler, J.; Fecteau-Lefebvre, A.; De Carlo, S.; Müller, E.; Goldie, K. N.; Regeni, I.; Li, T.; Santiso-Quinones, G.; Steinfeld, G.; Handschin, S.; van Genderen, E.; van Bokhoven, J. A.; Clever, G. H.; Pantelic, R. Rapid Structure Determination of Microcrystalline Molecular Compounds Using Electron Diffraction. *Angew. Chem., Int. Ed.* **2018**, *57* (50), 16313–16317.
- (23) Woollam, G. R.; Das, P. P.; Mugnaioli, E.; Andrusenko, I.; Galanis, A. S.; Van De Streek, J.; Nicolopoulos, S.; Gemmi, M.; Wagner, T. Structural Analysis of Metastable Pharmaceutical Loratadine Form II, by 3D Electron Diffraction and DFT+D Energy Minimisation. *CrystEngComm* **2020**, *22* (43), 7490–7499.
- (24) Lightowler, M.; Li, S.; Ou, X.; Zou, X.; Lu, M.; Xu, H. Indomethacin Polymorph δ Revealed To Be Two Plastically Bendable Crystal Forms by 3D Electron Diffraction: Correcting a 47-Year-Old Misunderstanding**. *Angew. Chem., Int. Ed.* **2022**, *61* (7), 1–7.
- (25) Rodriguez, J. A.; Ivanova, M. I.; Sawaya, M. R.; Cascio, D.; Reyes, F. E.; Shi, D.; Sangwan, S.; Guenther, E. L.; Johnson, L. M.; Zhang, M.; Jiang, L.; Arbing, M. A.; Nannenga, B. L.; Hattne, J.; Whitelegge, J.; Brewster, A. S.; Messerschmidt, M.; Boutet, S.; Sauter, N. K.; Gonen, T.; Eisenberg, D. S. Structure of the Toxic Core of α -Synuclein from Invisible Crystals. *Nature* **2015**, *525* (7570), 486–490.
- (26) Xu, H.; Lebrette, H.; Clabbers, M. T. B.; Zhao, J.; Griese, J. J.; Zou, X.; Högbom, M. Solving a New R2lox Protein Structure by Microcrystal Electron Diffraction. *Sci. Adv.* **2019**, *5* (8), 1–7.
- (27) Danelius, E.; Porter, N. J.; Unge, J.; Arnold, F. H.; Gonen, T. MicroED Structure of a Protoglobin Reactive Carbene Intermediate. *J. Am. Chem. Soc.* **2023**, *145* (13), 7159–7165.
- (28) Mugnaioli, E.; Andrusenko, I.; Schuler, T.; Loges, N.; Dinnebier, R. E.; Panthofer, M.; Tremel, W.; Kolb, U. Ab Initio Structure Determination of Vateite by Automated Electron Diffraction. *Angew. Chem., Int. Ed.* **2012**, *51* (28), 7041–7045.
- (29) Krysiak, Y.; Maslyk, M.; Silva, B. N.; Plana-Ruiz, S.; Moura, H. M.; Munsignatti, E. O.; Vaiss, V. S.; Kolb, U.; Tremel, W.; Palatinus, L.; Leitão, A. A.; Marler, B.; Pastore, H. O. The Elusive Structure of Magadiite, Solved by 3D Electron Diffraction and Model Building. *Chem. Mater.* **2021**, *33* (9), 3207–3219.
- (30) Krysiak, Y.; Plana-Ruiz, S.; Fink, L.; Alig, E.; Bahnmüller, U.; Kolb, U.; Schmidt, M. U. High Temperature Electron Diffraction on

Organic Crystals: *In Situ* Crystal Structure Determination of Pigment Orange 34. *J. Am. Chem. Soc.* **2024**, *146* (14), 9880–9887.

(31) Gorelik, T.; Schmidt, M. U.; Brüning, J.; Bekó, S.; Kolb, U. Using Electron Diffraction to Solve the Crystal Structure of a Laked Azo Pigment. *Cryst. Growth Des.* **2009**, *9* (9), 3898–3903.

(32) Schmidt, M. U.; Brühne, S.; Wolf, A. K.; Rech, A.; Brüning, J.; Alig, E.; Fink, L.; Buchsbaum, C.; Glinnemann, J.; Van De Streek, J.; Gozzo, F.; Brunelli, M.; Stowasser, F.; Gorelik, T.; Mugnaioli, E.; Kolb, U. Electron Diffraction, X-Ray Powder Diffraction and Pair-Distribution-Function Analyses to Determine the Crystal Structures of Pigment Yellow 213, C₂₃H₂₁N₅O₉. *Acta Crystallogr., Sect. B: Struct. Sci.* **2009**, *65* (2), 189–199.

(33) Wang, Y.; Takki, S.; Cheung, O.; Xu, H.; Wan, W.; Öhrström, L.; Inge, A. K. Elucidation of the Elusive Structure and Formula of the Active Pharmaceutical Ingredient Bismuth Subgallate by Continuous Rotation Electron Diffraction. *Chem. Commun.* **2017**, *53* (52), 7018–7021.

(34) Svensson Grape, E.; Rooth, V.; Smolders, S.; Thiriez, A.; Takki, S.; De Vos, D.; Willhammar, T.; Inge, A. K. Bismuth Gallate Coordination Networks Inspired by an Active Pharmaceutical Ingredient. *Dalton Trans.* **2022**, *51* (37), 14221–14227.

(35) Delgado Friedrichs, O.; O’Keeffe, M.; Yaghi, O. M. Three-Periodic Nets and Tilings: Regular and Quasiregular Nets. *Acta Crystallogr., Sect. A: Found. Crystallogr.* **2003**, *59* (1), 22–27.

(36) Fester, G. A. Einige Farbstoffe Südamerikanischer Kulturvolker. *Isis* **1953**, *44*, 13–16.

(37) *Artists’ Pigments: A Handbook of Their History and Characteristics*; Feller, R. L., Roy, A., FitzHugh, E. W., Berrie, B. H., Eds.; National Gallery of Art: 1986.

(38) Huang, Q.; Li, W.; Mao, Z.; Qu, L.; Li, Y.; Zhang, H.; Yu, T.; Yang, Z.; Zhao, J.; Zhang, Y.; Aldred, M. P.; Chi, Z. An Exceptionally Flexible Hydrogen-Bonded Organic Framework with Large-Scale Void Regulation and Adaptive Guest Accommodation Abilities. *Nat. Commun.* **2019**, *10* (1), 3074.

(39) Wang, Y.; Ma, K.; Bai, J.; Xu, T.; Han, W.; Wang, C.; Chen, Z.; Kirlikovali, K. O.; Li, P.; Xiao, J.; Farha, O. K. Chemically Engineered Porous Molecular Coatings as Reactive Oxygen Species Generators and Reservoirs for Long-Lasting Self-Cleaning Textiles. *Angew. Chem., Int. Ed.* **2022**, *134* (8), No. e202115956.